International Journal of Pharmaceutics: X 3 (2021) 100089

Contents lists available at ScienceDirect

International Journal of Pharmaceutics: X

journal homepage: www.sciencedirect.com/journal/international-journal-of-pharmaceutics-x

Oral etoposide and zosuquidar bioavailability in rats: Effect of co-administration and *in vitro-in vivo* correlation of P-glycoprotein inhibition

Rasmus Blaaholm Nielsen [a], René Holm [a,b], Ils Pijpers [c], Jan Snoeys [c], Ulla Gro Nielsen [a], Carsten Uhd Nielsen [a,*]

[a] Department of Physics, Chemistry and Pharmacy, University of Southern Denmark, Campusvej 55, DK-5230 Odense M, Denmark
[b] Drug Product Development, Janssen R&D, Johnson & Johnson, Turnhoutseweg 30, BE-2340 Beerse, Belgium
[c] Drug Metabolism and Pharmacokinetics, Janssen R&D, Johnson & Johnson, Turnhoutseweg 30, BE-2340 Beerse, Belgium

ARTICLE INFO

Keywords:
P-glycoprotein
Etoposide
Zosuquidar
Efflux transport
Oral absorption
Caco-2
in vitro-in vivo correlation

ABSTRACT

P-glycoprotein inhibitors, like zosuquidar, have widely been used to study the role of P-glycoprotein in oral absorption. Still, systematic studies on the inhibitor dose-response relationship on intestinal drug permeation are lacking. In the present study, we investigated the effect of 0.79 nM-2.5 μM zosuquidar on etoposide permeability across Caco-2 cell monolayers. We also investigated etoposide pharmacokinetics after oral or IV administration to Sprague Dawley rats with co-administration of 0.063–63 mg/kg zosuquidar, as well as the pharmacokinetics of zosuquidar itself. Oral zosuquidar bioavailability was 2.6–4.2%, while oral etoposide bioavailability was 5.5 ± 0.9%, which increased with increasing zosuquidar doses to 35 ± 5%. The intestinal zosuquidar concentration required to induce a half-maximal increase in bioavailability was estimated to 180 μM. In contrast, the IC_{50} of zosuquidar on etoposide permeability *in vitro* was only 5–10 nM, and a substantial *in vitro-in vivo* discrepancy of at least four orders of magnitude was thereby identified. Overall, the present study provides valuable insights for future formulation development that applies fixed dose combinations of P-glycoprotein inhibitors to increase the absorption of poorly permeable P-glycoprotein substrate drugs.

1. Introduction

Zosuquidar (also referred to as LY-335979 or RS-33295-198) is a third generation P-glycoprotein (P-gp) inhibitor developed in the mid 1990's for co-administration with chemotherapeutics to counteract multidrug resistance in cancer therapy (Dantzig et al., 1996; Slate et al., 1995). Zosuquidar is a competitive P-gp inhibitor that binds to the central binding pocket of P-gp (Alam et al., 2019; Alam et al., 2018; Nosol et al., 2020), and it has been the subject of several clinical trials (; Fracasso et al., 2004; Gerrard et al., 2004; Lancet et al., 2009; Le et al., 2005; Morschhauser et al., 2007; Rubin et al., 2002; Ruff et al., 2009; Sandler et al., 2004), including one phase III trial (Cripe et al., 2010). Although zosuquidar is not marketed as a P-gp inhibitor, it has been heavily utilised as a model inhibitor in the research of ADME properties of potential P-gp substrates. For instance, zosuquidar has commonly been applied to alter the distribution of P-gp substrates to the CNS by inhibition of P-gp mediated cellular efflux in the blood-brain barrier (Bihorel et al., 2007; Chen et al., 2009; Choo et al., 2000; Dai et al., 2003; Karssen et al., 2002; Mittapalli et al., 2012; Nagaya et al., 2020) and to a lesser extent to increase the oral absorption of P-gp substrates (Adane et al., 2012; Al-Ali et al., 2020; Bardelmeijer et al., 2004; Matsuda et al., 2013; Mouly et al., 2004; Kono et al., 2021; Tsukimoto et al., 2015). Recently, the influence of factors such as sex, dosing time, and food intake on P-gp expression and function in the small intestine has also been investigated (Dou et al., 2020; Mai et al., 2019; Mai et al., 2018; Mai et al., 2021), and zosuquidar has been applied as an inhibitor in this context as well (Kara et al., 2021). However, a thorough understanding of zosuquidar doses needed to increase oral absorption of P-gp substrates, as well as information about the pharmacokinetics of zosuquidar itself, are missing, and both are needed to apply zosuquidar in formulation design. In oral absorption studies, zosuquidar has been dosed at maximally two different doses, and consequently, systematic investigations of the dose-response relationship of zosuquidar on the oral absorption and oral pharmacokinetics of P-gp substrates are

* Corresponding author.
E-mail address: cun@sdu.dk (C.U. Nielsen).

https://doi.org/10.1016/j.ijpx.2021.100089
Received 3 July 2021; Accepted 3 July 2021
Available online 7 July 2021

lacking. For example, 20 mg/kg oral zosuquidar increased the oral bioavailability of etoposide from 4.0% to 34.5% (Al-Ali et al., 2020), which was significant, but still far from the 92% oral etoposide bioavailability reported in *mdr1a(−/−)* knockout rats (Al-Ali et al., 2018a). These findings indicated that a 20 mg/kg dose of zosuquidar did not completely inhibit the P-gp function. Therefore, systematic knowledge about the zosuquidar dose-response relationship may solidify the application of zosuquidar as a model P-gp inhibitor and thereby aid in the design of drug formulations that contain P-gp substrates.

As a result of the missing investigations mentioned above, the *in vitro-in vivo*-correlation of P-gp inhibition by zosuquidar is also lacking. Numerous studies have estimated the potency of zosuquidar as a P-gp inhibitor *in vitro* (Al-Ali et al., 2018b; Choo et al., 2000; Green et al., 2001; Heredi-Szabo et al., 2013; Ozgur et al., 2018a, 2018b; Shaik et al., 2007). However, it is still not clear which zosuquidar dose is needed *in vivo* to negate P-gp function in the intestine. Performing *in vitro-in vivo* correlation of zosuquidar effects on the pharmacokinetics of a P-gp substrate may contribute with novel understanding of the complex dynamics of interactions between substrate, inhibitor, and transporter in the small intestine. Therefore, we investigated the effect of increasing zosuquidar concentrations on the transcellular etoposide permeability across Caco-2 cell monolayers, as well as on the pharmacokinetics of etoposide in rats, and we correlated the observed *in vitro* and *in vivo* effects.

Additionally, the oral pharmacokinetics of zosuquidar itself is only sparsely described in the public domain with no estimates of absolute oral bioavailability. Zosuquidar has been reported to be rapidly cleared from the intestine in mice (Bardelmeijer et al., 2004), and the pharmacokinetics of zosuquidar in mice or rats may play a crucial role in the design of studies, where zosuquidar is used as a P-gp inhibitor. Therefore, systematic knowledge about zosuquidar pharmacokinetics is necessary to obtain a better understanding of the effects elicited by zosuquidar on the P-gp substrates in question. Accordingly, we investigated the pharmacokinetics of zosuquidar in rats and assessed the interplay between zosuquidar and etoposide pharmacokinetics.

2. Materials and methods

2.1. Materials

Ultrapure water was obtained from an in-house Milli-Q water purification system (Millipore, Burlington, MA, USA). Fetal Bovine Serum (Biowest) was from VWR (Radnor, PA, USA). Zosuquidar 3HCl and etoposide was from Medkoo (Morrisville, NC, USA). In the present publication, any given amount of 'zosuquidar' refers to the free molecule without the HCl salt component. All other chemicals were obtained from Merck (Darmstadt, Germany).

2.2. Cell culturing

Caco-2 cells were obtained from Deutsche Sammlung von Mikroorganismen und Zellkulturen (DSMZ). Caco-2 cells were seeded at a density of 1×10^5 cells per filter on polycarbonate filter inserts (1.12 cm^2, 0.4 μM pore size, Corning, Corning, NY, USA). Experiments were performed 14 days after seeding in a Transwell system. Cells were maintained in Dulbecco's modified eagle medium supplied with 10% fetal bovine serum, penicillin (100 U/ml), streptomycin (100 μg/mL), L-glutamine (2 mM), and non-essential amino acids (1×) under atmospheric air supplied with 5% CO_2 and 95% relative humidity (Heracell 150i incubator, Thermo Fisher Scientific, Waltham, MA, USA). Culture medium was changed three times per week.

2.3. Etoposide permeability across Caco-2 cell monolayers

Permeability experiments were carried out in three to four individual cell passages. Donor solutions containing etoposide and lucifer yellow were prepared in 10 mM HEPES HBSS pH 7.4 from a 20 mM etoposide stock in DMSO and a 2.6 mM lucifer yellow (lithium salt) stock in ultrapure water. Receiver solutions consisted of 10 mM HEPES HBSS. Zosuquidar solutions of 100 times the final apparent concentrations were prepared from a 10 mM zosuquidar stock in methanol for spiking.

The permeability of 50 μM etoposide was assessed in both the apical to basolateral (A-B) direction and in the basolateral to apical (B-A) direction without zosuquidar or in the presence of 0.79 nM-2.5 μM zosuquidar. Growth media was removed from the cells by vacuum suction (Vacusip, Integra Biosciences, Hudson, NH, USA), and the cells were equilibrated in 10 mM HEPES HBSS for 10 min on a Talboys 1000MP incubating microplate shaker (Troemner, West Deptford, NJ, USA, 220 rpm, 37 °C). Donor or receiver solutions were added with 495 or 990 μL in apical or basolateral wells, respectively. Immediately hereafter, all donor and receiver wells were spiked with 5 or 10 μL of a 100 times concentrated zosuquidar solution in the apical or basolateral wells, respectively. The resulting solutions contained 1% (v/v) methanol and 0.25% (v/v) DMSO.

Sampling was performed at 15, 30, 60, 90, and 120 min by taking a 50 μL sample that was immediately diluted 1:1 in methanol:water in an HPLC vial, and the sampled volume was replaced by 50 μL of the corresponding receiver solution. Donor samples were taken from the main donor solution at 0 min and at 120 min from each donor compartment. Both samples were diluted as described above and analysed by fluorescence-coupled HPLC (HPLC-FL) for both etoposide and zosuquidar. After HPLC-FL analysis, 50 μL of the remaining sample volume was transferred to a black, clear bottom 96-well plate (Corning, Corning, NY, USA) and analysed for lucifer yellow.

Etoposide and lucifer yellow flux across Caco-2 monolayers was calculated by linear regression of the accumulated amount permeated at steady-state (time 30–120 min), and the apparent permeability (P_{app}) was estimated by dividing with the donor concentration of etoposide. Etoposide recovery was 95–117% and lucifer yellow recovery was 82–110%. Etoposide efflux ratio for each apparent zosuquidar concentration was calculated by dividing the B-A P_{app} with the A-B P_{app}. Etoposide P_{app} was plotted against the apparent zosuquidar concentration and regression was performed in GraphPad Prism 8.4.0 using Eq. 1

$$Y = \text{Bottom} + \frac{\text{Top} - \text{Bottom}}{1 + \left(\frac{IC_{50}}{X}\right)^{\text{Hill Slope}}} \quad (1)$$

where Y is the etoposide P_{app}, X is the zosuquidar concentration, Bottom and Top are the low and high etoposide P_{app} plateaus, respectively, IC_{50} is the zosuquidar concentration at the midway point between low and high P_{app} plateaus, and the Hill Slope is the Hill Coefficient, determining the slope of the dose-response curve.

2.3.1. Zosuquidar recovery

During the studies, it was observed that zosuquidar in aqueous solutions tended to adsorb to plastic and glass surfaces, which interfered with the common practices for preparing solutions. For this reason, zosuquidar was added to cell culture plates at the start of the permeability studies by spiking the donor and receiver wells with concentrated zosuquidar solutions in methanol as described above. Furthermore, the zosuquidar recovery in solution was investigated when applied in i) the basolateral, ii) the apical compartment, iii) the cell layer, and iv) in the plastic of the cell culture plate. Zosuquidar recovery was determined for all wells containing 79, 250, 790 nM or 2.5 μM. For lower apparent concentrations, the lower limit of quantification (LOQ) of the HPLC-FL method was not sufficient to determine the zosuquidar recovery accurately. The zosuquidar concentration in the basolateral and apical compartment was assessed as described above under sampling during the permeability study. To assess zosuquidar content in the cell layer after the experiment, the filter containing the cell layer was cut out with a scalpel and transferred to a 1.5 mL low binding tube (Sarstedt, Newton,

NC, USA), and 500 µL 0.1% triton-X in 3:1 acetonitrile:water was added to extract zosuquidar and precipitate proteins. The filter and cell monolayer were then thoroughly mashed with a 1.5 mL Kimble pellet pestle (DWK Life Sciences, Rockwood, TN, USA) and shaken on a vertical rotator (10 rpm, PTR-60, Grant Instruments, Shepreth, UK) overnight. To assess zosuquidar content in the cell culture plate, 1.5 mL 57:43 methanol:35 mM ammonium acetate, pH 4.5 (zosuquidar HPLC-FL mobile phase) was added to each well and insert after the filter and cell layer was cut out. The plate was then incubated on an incubating microplate shaker for 1 h (room temperature, 220 rpm), and a sample of 1 mL was taken and transferred to a 1.5 mL micro tube. To sediment any precipitated protein, the cell layer and cell culture plate samples were centrifuged (15,000 RCF, 22 °C, 10 min, Multifuge X1R, Thermo Fisher Scientific, Waltham, MA, USA). Supernatant from the cell layer samples were diluted 1:2 in ultrapure water and analysed by HPLC-FL, and supernatant from cell culture plate samples were transferred and analysed directly by HPLC-FL.

Zosuquidar recovery was calculated for the four compartments as the absolute amount of zosuquidar present in each compartment, relative to the added amount of zosuquidar by spiking to start the experiment, while correcting for the amount removed by sampling and added by the replacement with relevant receiver media. The zosuquidar recovery values as a percentage for each well in both A-B and B-A experiments were then pooled.

2.3.2. Cell layer integrity assessment

The permeability of lucifer yellow at a concentration of 100 µM was utilised as a passive permeability marker. Lucifer yellow P_{app} was below 1.1×10^{-6} cm/s and was not affected by increasing concentrations of zosuquidar.

Before and after each experiment, transepithelial electrical resistance (TEER) was measured to assess cell monolayer integrity with an EVOM2 epithelial voltohmmeter connected to an Endohm 12 culture cup (World Precision Instruments, Sarasota, FL, USA). The TEER of Caco-2 cells before the experiments ranged from 557 to 747 $\Omega \times cm^2$ and dropped by 42% on average after the experiment. No single filter displayed a drop in TEER of more than 65% during the experiment. TEER measurements were consistent with previous in-house studies (Al-Ali et al., 2018a). Based on the TEER measurements and lucifer yellow P_{app}, all cell layers were considered intact, and treatments were not considered to affect cell layer integrity.

2.3.3. Etoposide and zosuquidar quantification by fluorescence-coupled HPLC

Etoposide and zosuquidar were quantified by HPLC-FL (Shimadzu, Kyoto, Japan). Etoposide was detected at an excitation wavelength of 230 nm and an emission wavelength of 330 nm and zosuquidar was detected at 240/415 nm excitation/emission with 'medium' sensitivity setting and ×4 gain. For etoposide, the mobile phase consisted of 38:61.5:0.5 methanol:ultrapure water:acetic acid, and for zosuquidar the mobile phase consisted of 57:43 methanol:35 mM ammonium acetate pH 4.5. 20 µL of the sample was injected and a flow rate of 0.3 mL/min was applied over a reversed phase column (XBridge C18 2.5 µM, 2.1 × 30 mm, Waters, Milford, MA, USA) kept at 40 °C. The retention time was 2.0 min for etoposide and 2.4 min for zosuquidar. The LOQ was 35 and 8 nM for etoposide and zosuquidar, respectively. Calibration standards were prepared in the respective mobile phase from a 20 mM etoposide stock solution in DMSO and a 10 mM zosuquidar stock solution in methanol. Calibration standards in the range 0.034–25 µM for etoposide and 0.008–2 µM for zosuquidar was prepared and analysed and linear regression with 1/x weighing was applied.

2.3.4. Lucifer yellow quantification

Lucifer yellow was quantified on a Fluostar Omega plate reader (BMG Labtech, Ortenberg, Germany) *via* the top optics with 440–10 nm excitation filter setting, 520 nm emission filter setting, and 200 flashes per well. A calibration curve was prepared by serial dilution in the plate ranging from 0.04 to 5 µM lucifer yellow. Linear regression was applied and LOQ was 0.04 µM.

2.4. Etoposide solubility in ethanol-water mixtures

Ethanol-water mixtures of 0, 10, 25, 40, 50, 60, 75, 90, and 100% *v*/v ethanol were prepared by addition of appropriate amounts of absolute ethanol to volumetric flasks and filling to volume with ultrapure water. 2–6 mg etoposide was weighed in individual 1.5 mL LowBind tubes (Sarstedt, Newton, NC, USA). 500 µL ethanol-water mixture was added to each tube, and the tubes were shaken on a vertical rotator (10 rpm) for approximately 24 h at ambient temperature (20–22 °C). Visual inspection confirmed that there was undissolved etoposide in all tubes. Subsequently, the tubes were centrifuged (25,000 RCF, 15 min, 22 °C, Multifuge X1R, Thermo Fisher Scientific, Waltham, MA, USA) and a 10 µL aliquot of the supernatant was diluted in etoposide mobile phase and analysed by HPLC-FL.

2.5. Pharmacokinetic dose escalation study in rats

The study was conducted according to the European convention for the protection of vertebrate animals used for experimental and other scientific purposes (ETS no. 123, Directive 2010/63/EU) and Belgian law controlling the experiments on animals (Royal Decree of May 29, 2013 for the protection of laboratory animals). The study was performed under the following ethical protocols: ECD project: Project 027-Early PK, ECD procedure: 138-Absorption.

2.5.1. Formulation stability and pH

To assess precipitation and pH upon dilution in rat intestinal fluid, formulations were diluted with a modified rat simulated intestinal fluid (rSIF) based on the rSIF reported by Berghausen et al. (2016). The modified rSIF contained 25 mM sodium taurocholate, 5.16 mM lecithin, 30 mM maleic acid, 19 mM NaCl and was adjusted to pH 6.0 with NaOH. Formulations were diluted 1:1 in rSIF and precipitation upon dilution was assessed visually. The pH of the administered zosuquidar-containing formulations were 2.7, 6.5, 4.3, 3.6, 3.2, 2.7, and 2.2, and pH values after dilution in rSIF were 6.4, 6.8, 6.8, 6.8, 6.7, 6.4, and 4.4 (groups B, E, F, G, H, I, and J, respectively, Table 1). For 2.0 and 6.3 mg/mL zosuquidar (groups B, I, J, Table 1), precipitation was observed, but all dilutions of lower zosuquidar concentrations remained clear. Etoposide did not precipitate from any formulation. For the precipitated rSIF-formulation mixtures, the suspension was centrifuged (25,000 RCF, 37 °C, 5 min, Multifuge X1R, Thermo Fisher Scientific, Waltham, MA, USA), and the supernatant was sampled and diluted 100 times in zosuquidar mobile phase and analysed by HPLC-FL. The resulting initial solubilities for formulations B, I, and J were 0.45, 0.52, and 0.47 mg/mL zosuquidar, corresponding to 44, 52, and 15% of the dose strength being in solution.

2.5.2. Dosing

Male Sprague Dawley rats with a mean weight of 303 g ± 12 g on the day of administration were randomly divided into ten groups of six animals and dosed according to Table 1. The animals were acclimatized minimum 5 days in groups of 6 in polysulphone cages (floor surface = 58 × 52 × 20 cm = 3016 cm^2 / rodent retreat) and wooden sticks provided as enrichment. The animals were housed in buildings with controlled environmental conditions with a temperature of 22 ± 2 °C, relative humidity of 55 ± 10%, and a light cycle of 12 h. Animals had free access to Safe 04 Maintenance Diet (Safe, Rosenberg, Germany) and water throughout the entire study.

Intravenous (IV) administration was performed by injecting 2.5 mL/kg solution into the saphenous vein with a syringe using a 27G needle. Oral administration was performed by oral gavage of 10 mL/kg solution. For groups A-C, where solutions were administered both IV and orally,

Table 1
Study design overview.

Group description	IV Etoposide		IV Etoposide + Oral Zosuquidar		IV Zosuquidar		Oral Etoposide	Oral Etoposide + Zosuquidar Dose Escalation					
Group	A		B		C[a]		D	E	F	G	H	I	J
Administration route	Oral	IV	Oral	IV	Oral	IV	Oral	Oral	Oral	Oral	Oral	Oral	Oral
Administered volume (mL/kg)	10	2.5	10	2.5	10	2.5	10	10	10	10	10	10	10
Etoposide dose (mg/kg)	–	5	–	5	–	–	20	20	20	20	20	20	20
Zosuquidar dose (mg/kg)	–	–	20	–	–	5	–	0.063	0.63	2	6.3	20	63
Ethanol conc. (% v/v)	30	40	30	40	30	40	40	40	40	40	40	40	40

[a] Three of six animals died shortly after IV administration.

the oral administration was administered 3–5 min before the IV administration, and the sampling timer was started at the IV dose. The ethanol concentration in oral and IV administrations was adjusted so that all groups received the same total dose of ethanol. For all groups, plasma sampling was performed at 15, 30, 45 min, 1, 2, 3, 4, and 6 h. For groups A-C with IV administration, an additional plasma sampling was performed at 5 min. Blood sampling was performed by tail vein puncture into Micro haematocrit tubes 32–64 µL EDTA (Vitrex Medical, Herlev, Denmark) and plasma was centrifuged and transferred into 10 µL end-to-end pipettes for the bioanalysis (Vitrex Medical, Herlev, Denmark) and immediately frozen at −80 °C until analysis. At the end of the study, the animals were euthanised based upon the principles of euthanasia stated in the AVMA Guidelines for the Euthanasia of Animals (American Veterinary Medical Association, 2020).

2.5.3. Bioanalysis

Plasma samples of the etoposide- and zosuquidar-dosed groups were analysed using a qualified LC-MS/MS method. The capillary samples were washed out with 10 parts of 2% BSA in PBS pH 7.5 prior to further sample preparation. All samples were subjected to protein precipitation with acetonitrile, followed by LC-MS. Calibration standards for etoposide and zosuquidar and quality control to cover the calibration range were prepared in rat plasma. Calibration standards, quality control samples and study samples were processed at the same time. The peak area of the analyte was plotted against the analyte concentrations, and a linear regression model with $1/x^2$ weighing was used. LOQ was 4 ng/mL for etoposide and 0.2 ng/mL for zosuquidar.

LC-MS/MS analysis were carried out on a Triple Quad 6500+ mass spectrometer (Sciex, Danaher Corporation, DC, USA), which was coupled to an HPLC system (Shimadzu, Kyoto, Japan). Sample extracts were injected onto an Acquity UPLC BEH C18 1.7 µm 2.1 × 50 mm HPLC column (Waters, Milford, MA, USA) kept at 50 °C. Mobile phases consisted of 0.01 M ammonium acetate in water and acetonitrile, starting at 5% acetonitrile, held for 0.25 min followed by a gradient to 95% acetonitrile over 1.25 min.

For etoposide, the MS operated in the negative ion mode using the TurboIonSpray™-interface (electrospray ionization) and was optimized for the quantification of etoposide (MRM transition *m/z* 587.2 > 381). For zosuquidar, the MS operated in the positive ion mode and was optimized for the quantification (MRM transition m/z 528.2 > 241).

2.5.4. Data analysis

All pharmacokinetic parameters were calculated individually for each animal and then pooled in groups for graphing and statistical analysis. For IV curves of etoposide, the initial plasma concentration was estimated by linear regression of the ln(plasma concentration) *versus* time from 5 to 15 min. For IV zosuquidar (group C), the pharmacokinetic profile was fitted to a two-compartment elimination model consisting of two exponential terms:

$$Y = a \times e^{k_{e1} \times X} + b \times e^{k_{e2} \times X} \quad (2)$$

where Y is the plasma concentration, X is time after dosing, k_{e1} is the initial elimination rate, k_{e2} is the terminal elimination rate, and a and b are the initial plasma concentrations for each exponential term, respectively. The initial plasma concentration of zosuquidar was a + b.

The area under the curve (AUC) was calculated in GraphPad Prism 8.4 after inserting the estimated initial plasma concentration for IV curves (groups A-C) and 0 ng/mL for the oral curves (groups D-J) at 0 min. Each $AUC_{0\text{-}6h}$ was then normalised by dividing with the dose of etoposide or zosuquidar administered. Absolute bioavailability was then calculated by dividing the dose-corrected $AUC_{0\text{-}6h}$ by the mean dose-corrected $AUC_{0\text{-}6h}$ of a control IV group (group A for etoposide, and group C for zosuquidar, Table 1). For IV and oral etoposide as well as oral zosuquidar administrations, the elimination rate constant was calculated by linear regression on the linear part of the ln(plasma concentration) *vs.* time, and the plasma half-life ($t_{½}$) was calculated:

$$t_{½} = \frac{ln(2)}{k_e} \quad (3)$$

For IV curves of etoposide and zosuquidar, the systemic clearance (CL) was calculated:

$$CL = \frac{Dose}{AUC_{0-6h}} \quad (4)$$

Finally, log-linear regression was performed on the etoposide bioavailability (Y) *vs.* the orally co-administered zosuquidar dose (X):

$$Y = log(X) \times a + b \quad (5)$$

2.5.5. Statistical analysis

Descriptive statistics were calculated in GraphPad Prism 8.4. Etoposide bioavailability, the initial plasma concentration (C_{15min}), C_{max} and $t_{½}$ were compared to group D (Table 1) by one-way ANOVA followed by a Dunnett's test. All *P*-values below 0.05 were considered statistically significant.

3. Results and discussion

3.1. Zosuquidar accumulated in Caco-2 cell monolayers and cell culture plates

Zosuquidar is a highly lipophilic weak base (CLogP = 4.8, predicted pK_a = 7.6 (Drugbank, 2021)). Preliminary observations suggested that zosuquidar adhered to both glass and various plastic surfaces. Therefore, the free zosuquidar concentration in solution in the cell culture plates and inserts, as well as the amount accumulated in the Caco-2 cell monolayer, during the etoposide permeability study was investigated. The free zosuquidar concentration in the receiver compartments (both apical and basolateral) was reduced by 60–72% (data not shown) after only 30 min, and only 1.55 ± 0.06 and 7.01 ± 0.37% was left in solution after 120 min in the apical and basolateral compartment, respectively (Fig. 1B). Furthermore, zosuquidar recovery was 58.7 ± 5.0% in the Caco-2 monolayer and 31.8 ± 11.3% in the cell culture plate. Considering the high lipophilicity of zosuquidar, the accumulation of zosuquidar into the Caco-2 cell monolayer was most likely due to cell membrane accumulation.

The zosuquidar cell membrane accumulation may theoretically lead to increased zosuquidar mediated P-gp inhibition, as zosuquidar was accumulated at the site of the transporter. Conversely, the adsorption of

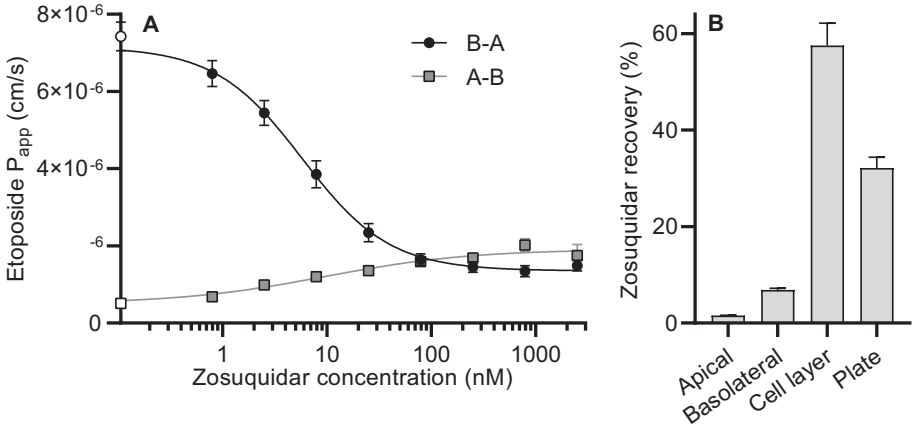

Fig. 1. A) Apparent permeability of 50 μM etoposide across Caco-2 cells in the apical-to-basolateral (A-B) and the basolateral-to-apical (B-A) direction at a zosuquidar concentration of 0.79 nM-2.5 μM. The permeability of etoposide without zosuquidar (control) is plotted on the y-axis for comparison (open symbols). The lines depict non-linear dose response regression (Eq. 1). Shown as mean ± SEM, $n = 4$ for B-A and 3 for A-B, SEMs smaller than the symbol size are not shown. B) Recovery of zosuquidar in solution in the apical or basolateral compartment, in the cell monolayer, or in the cell culture plate at 120 min. Expressed as % of added zosuquidar, corrected for sampling and replacement during the experiment. Pooled data shown for A-B and B-A studies with an apparent zosuquidar concentration of 79, 250, 790 nM or 2.5 μM over three independent cell passages. Expressed as mean ± SEM, $n = 3$ cell passages × 4 concentrations × 2 (A-B + B-A) = 24.

zosuquidar onto the cell culture plate would theoretically lead to a lowered effect of zosuquidar on P-gp-mediated efflux. However, neither effect was observable in the etoposide flux curves, where all flux curves were linear from 15 min with no apparent tendency to flatten or steepen during the experiment (not shown).

Other studies have shown that the presence of serum abolished activity of some well-known P-gp modulators *in vitro* (Lehnert et al., 1996; Ludescher et al., 1995), probably by protein binding and subsequent lowering of free modulator concentrations. The present zosuquidar accumulation data illustrates that care must be taken in the design and interpretation of *in vitro* studies that applies zosuquidar or other compounds that tends to bind to protein, plastic or similar.

3.2. Zosuquidar abolished the polarisation of etoposide permeability in Caco-2 cell monolayers

The bidirectional permeability of etoposide in the presence of increasing zosuquidar concentrations and estimated kinetic parameters are shown in Fig. 1 and Table 2, respectively. In the absence of zosuquidar, etoposide P_{app} showed a B-A polarised transport with an efflux ratio of 15.4 ± 1.3. Similar etoposide efflux ratios have been reported and was the result of P-gp-mediated efflux of etoposide (Al-Ali et al., 2018a; Guo et al., 2002; Makhey et al., 1998). The minimum apparent zosuquidar concentration necessary to abolish P-gp mediated etoposide efflux was 79 nM (Fig. 1A). Increasing the applied zosuquidar concentration to 2.5 μM maintained the efflux ratio at approximately one. Thus, the presence of 79 nM-2.5 μM zosuquidar was required *in vitro* to fully inhibit P-gp mediated etoposide efflux. Additionally, the polarised permeability of etoposide was slightly asymmetric as A-B permeability increased 4-fold and B-A permeability decreased 5-fold in the presence of more than 79 nM zosuquidar. This asymmetry has been reported for many P-gp substrates in both absorptive and secretory directions (Troutman and Thakker, 2003), and could point towards involvement of an unknown basolateral carrier or transporter of etoposide.

The estimated apparent IC_{50} of zosuquidar on P-gp mediated efflux of etoposide was 5.80 ± 1.70 nM for secretory etoposide transport and 9.50 ± 5.61 nM for the absorptive etoposide transport (Table 2). The IC_{50} of zosuquidar on bi-directional etoposide permeability has not been reported before, to our knowledge. In other cell lines with different substrates, estimated IC_{50}-values of zosuquidar on P-gp-mediated efflux includes 70 nM in MDCKII-MDR1 cells with abacavir as substrate (Shaik et al., 2007), 50 nM and 40 nM in IPEC-J2 MDR1 cells with digoxin and rhodamine-123 as substrates, respectively (Ozgur et al., 2018a, 2018b), and 24 nM in Caco-2 cells with digoxin as a substrate (Choo et al., 2000). Both substrate and enzyme concentrations affect the estimation of the IC_{50} value, so some variation was expected. However, the finding that zosuquidar adsorbs to various surfaces may also contribute to inter-laboratory variation given that the handling of zosuquidar in buffered aqueous solutions pose an additional challenge when preparing solutions for transcellular permeability experiments. Spiking the individual cell culture plate wells with concentrated zosuquidar solutions in methanol, like in the current study, should yield a relative accurate estimation of zosuquidar effects on P-gp function. In conclusion, the present study solidified that zosuquidar is a highly potent P-gp inhibitor.

3.3. Etoposide solubility in ethanol-water mixtures

For the preparation of oral etoposide solutions for animal dosing, we investigated the solubility of etoposide in various ethanol-water mixtures (Fig. 2). In pure water, the solubility was 0.0924 ± 0.0034 mg/mL, and in absolute ethanol, it was 0.891 ± 0.008 mg/mL. The highest solubility of etoposide was observed in 75% v/v ethanol, where it was 9.23 ± 0.42 mg/mL. For oral administrations in the *in vivo* study, the administered solutions were prepared with 2.0 mg/mL etoposide in a 40% v/v ethanol, where the etoposide solubility was 3.01 ± 0.03 mg/mL.

3.4. Zosuquidar pharmacokinetics

We examined the pharmacokinetics of etoposide and zosuquidar in Sprague Dawley rats after oral co-administration. As zosuquidar is a specific P-gp inhibitor, it was expected to elicit significant effects on etoposide pharmacokinetics, but it was also assumed that etoposide would *not* affect zosuquidar pharmacokinetics significantly, since

Table 2
In vitro regression parameters.

	Bottom (×10^{-6} cm/s)	Top (×10^{-6} cm/s)	IC_{50} (nM)	Hill Slope	R^2
B-A	1.35 ± 0.02	7.16 ± 0.65	5.80 ± 1.70	−1.04 ± 0.24	0.959
A-B	0.498 ± 0.110	1.91 ± 0.14	9.50 ± 5.61	0.615 ± 0.199	0.847

Obtained regression parameters (Eq. 1) of etoposide P_{app} against the zosuquidar concentration in the basolateral(B)-apical(A) direction ($n = 4$) and in the A-B direction ($n = 3$).

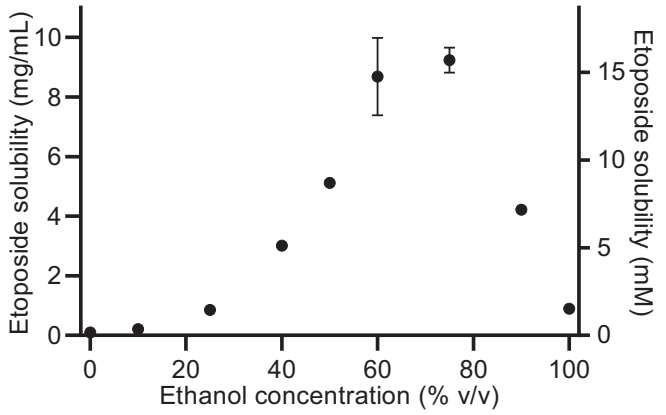

Fig. 2. Etoposide solubility in ethanol-water mixtures at ~22 °C. Shown as mean ± SD ($n = 3$), SDs smaller than the symbol size are not shown.

zosuquidar is an inhibitor of P-gp and not a substrate. This assumption has proven true in clinical trials. For example, were zosuquidar pharmacokinetics unaltered by combinatory chemotherapy with vincristine, doxorubicin, cyclophosphamide, and prednisolone (CHOP regimen) (Morschhauser et al., 2007).

The pharmacokinetic profile after IV administration of 5 mg/kg zosuquidar (Fig. 3) could be modelled by a two-compartment pharmacokinetic model with an initial log-linear distribution phase from 5 min to 15–30 min and a terminal log-linear elimination phase from 1 to 6 h. The $t_{½}$ of zosuquidar was 4.50 ± 0.56 min in the initial distribution phase and 140 ± 24 min in the terminal elimination phase (Table 3).

The pharmacokinetic profiles of zosuquidar after oral administration are shown in Fig. 4. For 0.063 mg/kg zosuquidar co-administration, the obtained plasma concentrations at some time points were below the LOQ (0.2 ng/mL) of the applied bioanalytical method, and this group was therefore not included in the analysis. The $AUC_{0\text{-}6h}$ of orally administered zosuquidar was highly dependent on the zosuquidar dose. The absolute bioavailability of zosuquidar varied between 2.58 ± 0.23 and 4.21 ± 0.81% (Table 3). The $t_{½}$ of zosuquidar after oral administration was in the range 82.0 ± 5.5 to 238 ± 14 min (Table 3).

In vitro, when the formulations with 2.0 or 6.3 mg/mL zosuquidar (groups B, I, and J) were diluted 1:1 in modified rSIF, precipitation was observed and may therefore also occur *in vivo*. Zosuquidar precipitation was, however, not evident in the obtained bioavailabilities as bioavailability was relatively constant over the different dosing groups.

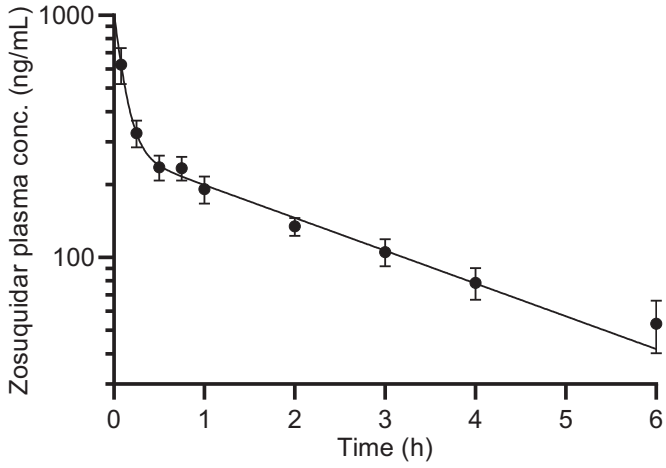

Fig. 3. Pharmacokinetic profile of zosuquidar after administration of 5 mg/kg zosuquidar IV bolus. Logarithmic y-axis. Shown as mean ± SEM, $n = 3$. The line represents a two-compartment model fit (Eq. 2).

The pH of the formulations before and after dilution showed as expected that, the presence of increasing zosuquidar concentrations lowered pH from 6.5 to 2.2. However, upon dilution in modified rSIF, the pH was 6.4–6.8 across all formulations, except for the highest dose of zosuquidar, where the pH was 4.4. The measured pH of a corresponding 1:1 mixture of 40% ethanol and rSIF was 6.8, which explained the apparent pH increase upon mixing. Still, despite different pH of the formulations, the rSIF had enough buffering capacity to buffer the formulations, except for the highest dose of 63 mg/kg zosuquidar. However, neither precipitation nor differing pH values of the formulations seemed to significantly affect zosuquidar bioavailability, as it was in the same range for all zosuquidar groups, regardless of the administered concentration. According to the predicted zosuquidar pK_a of 7.6, zosuquidar would exist primarily on protonated form in these pH ranges, which may have limited zosuquidar permeation and thereby contributed to the low observed bioavailability.

As indicated in Table 1, three of six animals who received the 5 mg/kg IV zosuquidar dose died shortly after administration. This was surprising given that 20 mg/kg zosuquidar IV was dosed in a previous study with no reported issues (Anderson et al., 2006). Animals were dosed with high doses of ethanol in the present study to ensure solubilisation of the administered compounds, but no animals in groups A and B, which received the same ethanol dose IV or orally, died or showed severe symptoms of intoxication during the study (Table 1). Thus, zosuquidar and ethanol may have potentiated the toxic effect of each other, which is important to note for the design of any future studies.

Estimates of absolute bioavailability of zosuquidar after oral administration are not available in the public domain. Generally, there are very few available data on zosuquidar pharmacokinetics with less than a handful of studies in mice or rats, and there are some data sets from clinical studies that reported plasma levels of zosuquidar after various dosing schemes (Fracasso et al., 2004; Lancet et al., 2009; Le et al., 2005; Morschhauser et al., 2007; Rubin et al., 2002; Sandler et al., 2004). Thereby, the presented absolute zosuquidar bioavailabilities in the present study are the first ones reported, and together with the pharmacokinetic parameters of zosuquidar, they contribute with novel information for the formulation development using zosuquidar to increase bioavailability poorly permeable P-gp substrate drugs. For comparison, zosuquidar plasma concentrations were reported in female Sprague Dawley rats after IV administration of 2, 6, and 20 mg/kg (Anderson et al., 2006), with reported zosuquidar plasma concentrations of approximately 1 μg/mL at 2 h after a 6 mg/kg IV bolus. In contrast, the zosuquidar plasma concentration in the present study was only 0.13 μg/mL 2 h after a 5 mg/kg IV bolus. Zosuquidar pharmacokinetics after oral administration in man are highly variable, and t_{max} is typically reported in the range of 1–4 h depending on the dose. $t_{½}$ also varies in the different reported studies as a function of dose and administration route from approx. 6–24 h (Le et al., 2005; Morschhauser et al., 2007). A high level of zosuquidar metabolism in hepatic microsomes from both rat, dog, monkey, and human have been reported (Ehlhardt et al., 1998), and zosuquidar seems to undergo a high level of first-pass metabolism upon oral administration in man (Rubin et al., 2002). Zosuquidar CL after IV administration was 102 ± 12 mL/min/kg in the present study, which exceeded the hepatic artery and portal vein blood flow of 67 mL/min/kg reported in adult rats (Delp et al., 1998). This also indicated extensive hepatic metabolism of zosuquidar, and that other elimination pathways are likely involved as well. Conclusively, oral zosuquidar bioavailability was found to be quite low in the present study, and the reported absolute zosuquidar bioavailability as well as the pharmacokinetic profiles after a single oral dose in the present study, contributes with new valuable knowledge for researchers designing studies in rats, where zosuquidar is applied as a model P-gp inhibitor.

Low bioavailability has also been reported for the intestine-specific P-gp inhibitor, encequidar (HM30181) (Kwak et al., 2010; Paek et al., 2006; Smolinski et al., 2021). Low oral bioavailability of encequidar was a key feature in the development to ensure a local intestinal effect with

Table 3
Pharmacokinetic parameters of etoposide and zosuquidar after oral or IV administration to male Sprague Dawley rats.

Group	A	B	C	D	E	F	G	H	I	J
Etoposide										
Adm. route	IV	IV	–	Oral	Oral	Oral	Oral	Oral	Oral	Oral
Dose (mg/kg)	5.0	5.0		20	20	20	20	20	20	20
$AUC_{0\text{-}6h}$ (μg/mL×h)	4.30±0.25	5.75±0.30		0.947±0.156	0.859±0.081	2.47±0.44	3.86±0.50	4.27±0.47	3.53±0.46	5.96±0.91
Bioavailability (%)	–	134±7		5.51±0.91	4.99±0.47	14.4±2.5*	22.4±2.9*	24.8±2.7*	20.5±2.7*	34.7±5.3*
C_{15min} (μg/mL)	–	–		0.381±0.082	0.541±0.058	1.29±0.16*	1.62±0.26*	1.69±0.18*	1.44±0.15*	2.15±0.34*
C_{max} (μg/mL)	–	–		0.390±0.084	0.563±0.067	1.59±0.29*	2.24±0.54*	2.11±0.20*	1.66±0.17*	2.53±0.34*
t_{max} (min)	–	–		15[15;30]	30[30;45]	45[30;45]	38[26;60]	45[15;60]	38[26;49]	38[26;45]
$t_{½}$ (min)	30.3±0.8	41.6±1.3		80.8±13.2	57.4±4.9	39.3±3.0*	51.4±2.4*	56.5±4.8*	60.7±5.4	74.9±4.0
CL (mL/min/kg)	19.7±1.1	14.7±0.8		–	–	–	–	–	–	–
Zosuquidar										
Adm. route	–	Oral	IV	–	Oral	Oral	Oral	Oral	Oral	Oral
Dose (mg/kg)		20	5.0		0.063	0.63	2.0	6.3	20	63
$AUC_{0\text{-}6h}$ (ng/mL×h)		94.2±12.4	830±87		BLQ	4.45±0.86	8.67±0.77	43.6±5.4	118±21	436±91
Bioavailability (%)		2.81±0.37	–			4.21±0.81	2.58±0.23	4.12±0.51	3.52±0.62	4.12±0.86
C_{max} (ng/mL)		23.7±3.6	–			1.34±0.28	2.10±0.27	10.9±1.2	31.3±3.2	105±21
t_{max} (min)		120[60;135]	–			120[101;120]	120[45;135]	90[45;120]	53[30;75]	60[45;120]
$t_{½}$ terminal (min)		173±10	140±24			82.0±5.5	217±27	161±13	194±23	238±14
$t_{½}$ initial (min)		–	4.50±0.56				–	–	–	–
CL (mL/min/kg)		–	102±12				–	–	–	–

Area under the curve from 0 to 6 h ($AUC_{0\text{-}6h}$), bioavailability, plasma concentration at 15 min (C_{15min}), maximal plasma concentration (C_{max}), and plasma half-life ($t_{½}$) given as mean ± SEM, t_{max} given as median [Q1;Q3], ($n = 6$, except for group C: $n = 3$). For etoposide parameters: Bioavailability, C_{15min}, C_{max}, and $t_{½}$ compared to control (group D) by one-way ANOVA followed by a Dunnett's test, significant difference ($p < 0.05$) marked by *. BLQ = zosuquidar content in plasma samples were below LOQ.

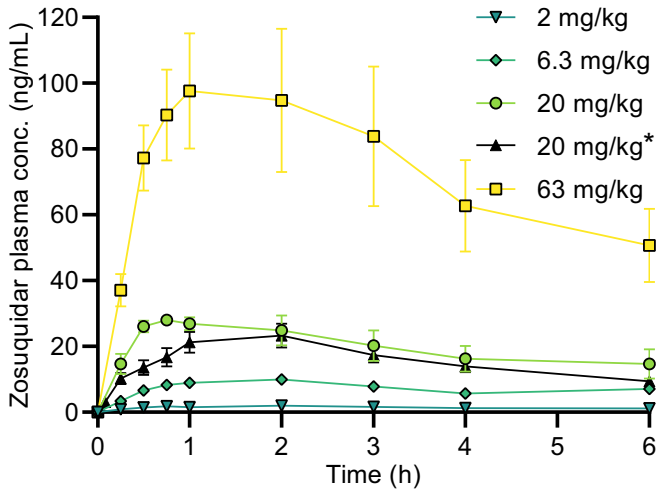

Fig. 4. Pharmacokinetic profiles of zosuquidar in male Sprague-Dawley rats after zosuquidar was co-administered alongside oral (20 mg/kg) or IV* (5 mg/kg) etoposide. Zosuquidar doses of 2.0, 6.3, 20, or 63 mg/kg. Shown as mean ± SEM, $n = 6$, SEMs smaller than the symbol size are not shown, straight connecting lines for illustrative purposes.

minimal systemic effects, and was emphasised as a potential advantage over other P-gp inhibitors, like tariquidar, elacridar, and zosuquidar (Smolinski et al., 2021). However, in the present study, zosuquidar elicited similar oral absorption to encequidar with bioavailabilities of 4.12 and 6.25%, respectively, as well as C_{max} values of 10.9 and 7.1 ng/mL after 6.3 mg/kg zosuquidar and 10 mg/kg encequidar, respectively (Smolinski et al., 2021). This shows that zosuquidar may still be a relevant compound for increasing the oral bioavailability of P-gp substrates.

3.5. Etoposide pharmacokinetics after zosuquidar dose escalation in rats

The pharmacokinetic profiles of etoposide after IV administration is shown in Fig. 5. Elimination followed first order kinetics. As shown, the elimination of etoposide was significantly decreased by an oral dose of 20 mg/kg zosuquidar as etoposide $AUC_{0\text{-}6h}$ and $t_{½}$ increased by 34 and 37%, respectively (Table 3).

Intestinal excretion mediated by P-gp have been reported to contribute to the clearance of etoposide, as approximately 10% of the administered etoposide dose was found unchanged in the intestine in FVB mice, whereas only approximately 2% was found unchanged in *Abcb1a/1b(−/−)* knockout mice (Lagas et al., 2010). In another study in rats, zosuquidar plasma concentrations above 270 ng/mL after a 2 mg/kg IV administration only lead to a very minor increase in the brain: plasma ratio. Therefore, it was deemed unlikely that the C_{max} of only 23.7 ± 3.6 ng/mL zosuquidar after an oral dose of 20 mg/kg zosuquidar (Table 3, group B) in the present study would contribute to any significant effects on etoposide pharmacokinetics as a result of systemic exposure of zosuquidar. Thus, the decrease in etoposide clearance after IV administration and oral zosuquidar co-administration could have

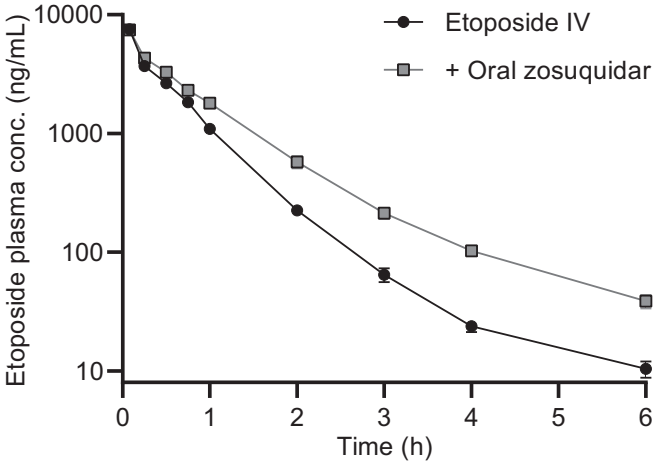

Fig. 5. Pharmacokinetic profile of etoposide after administration of 5 mg/kg etoposide IV and after co-administration of 5 mg/kg etoposide IV and 20 mg/kg zosuquidar orally. Logarithmic y-axis. Shown as mean ± SEM (n = 6), SEMs smaller than the symbol size are not shown, straight connecting lines for illustrative purposes.

been caused by a decreased intestinal excretion as a result of high zosuquidar concentrations in the small intestines. As zosuquidar bioavailability could be limited by first-pass metabolism, as described above, it was also likely that zosuquidar could affect hepato-biliary excretion of etoposide, despite low zosuquidar plasma concentrations after oral administration.

Orally administered etoposide showed a low oral bioavailability, a low C_{max}, and an early t_{max} of 15 min (Table 3). The pharmacokinetic profile of etoposide was altered by the co-administration of zosuquidar doses above 0.063 mg/kg. When compared to etoposide dosed without zosuquidar, bioavailability and C_{max} increased by 161 and 308%, respectively, both in a statistically significant manner, after co-administration of just 0.63 mg/kg zosuquidar. t_{max} tended to increase as well after co-administration of all applied zosuquidar doses above 0.063 mg/kg (Fig. 6, Table 3). Similarly, a statistically significant increase in bioavailability, C_{15min} and C_{max} was observed for all doses of oral zosuquidar co-administration above 0.063 mg/kg.

The absolute etoposide bioavailability increased with the dose of co-administered zosuquidar in an apparent log-linear manner (Fig. 7). In the case of 20 mg/kg zosuquidar co-administration, the bioavailability increased in a statistically significant manner to 20.5 ± 2.7%, however, it was lower than the groups that received 6.3 and 2.0 mg/kg zosuquidar co-administrations. Al-Ali et al. (2020) conducted a study under similar conditions in the same facilities, where 20 mg/kg etoposide was dosed orally in 7 mL/kg 57% ethanol, corresponding to the same dose of etoposide and ethanol as in the present study. The resulting etoposide bioavailability was 34.5 ± 0.2% (shown as a square in Fig. 7). The bioavailability of etoposide from Al Ali et al. and the present study dosed with 20 mg/kg zosuquidar individually deviates slightly from the correlation, but collectively follow the log-linear relationship.

The 63 mg/kg co-administered dose of zosuquidar resulted in an etoposide bioavailability of 34.7 ± 5.3%, which was still far below the 92% absolute etoposide bioavailability reported in P-gp knockout rats (Al-Ali et al., 2018a). However, Al-Ali et al. also reported that the absolute etoposide bioavailability was 27 ± 5% in wild-type rats compared to 5.51 ± 0.91% in the present study, which makes direct comparisons challenging. Nonetheless, since there was a noticeable increase in bioavailability after co-administration of 63 mg/kg zosuquidar compared to 6.3 and 20 mg/kg zosuquidar, it may be possible that doses above 63 mg/kg may increase the absolute etoposide bioavailability even further.

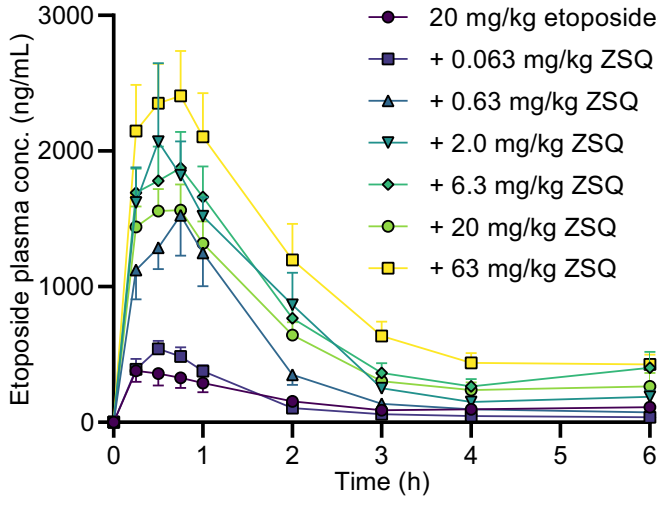

Fig. 6. Pharmacokinetic profiles of etoposide in male Sprague-Dawley rats after oral administration of 20 mg/kg etoposide and oral co-administration of 0.063, 0.63, 2.0, 6.3, 20, or 63 mg/kg zosuquidar (ZSQ). Shown as mean + or - SEM, n = 6, SEMs smaller than the symbol size are not shown, straight connecting lines for illustrative purposes.

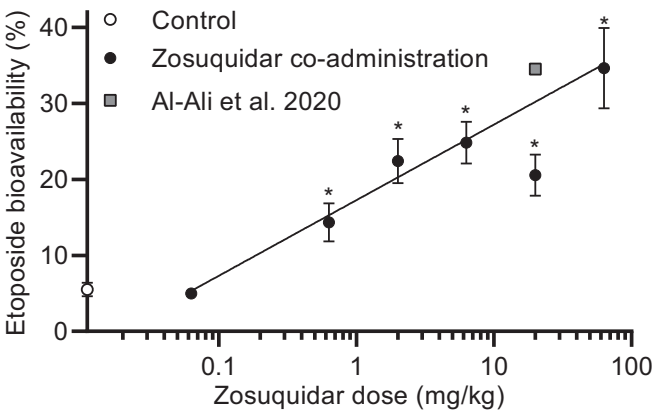

Fig. 7. Absolute etoposide bioavailability in male Sprague-Dawley rats after oral administration of 20 mg/kg etoposide as a function of the dose of orally co-administered zosuquidar. The control group dosed with 20 mg/kg etoposide without zosuquidar is plotted on the y-axis for comparison. Significantly different from 20 mg/kg etoposide (*, $p < 0.05$) according to one-way ANOVA followed by a Dunnett's test. The line represents log-linear regression (Eq. 5), where 20 mg/kg zosuquidar was not included ($R^2 = 0.656$). Etoposide bioavailability after oral co-administration of 20 mg/kg etoposide and 20 mg/kg zosuquidar from Al-Ali et al., 2020 reprinted for comparison. Shown as mean ± SEM, n = 6, SEMs smaller than the symbol size are not shown.

C_{15min} and C_{max} also tended to increase with increasing doses of co-administered zosuquidar, indicating increased absorption. The elimination of etoposide was lowest for the control group of 20 mg/kg oral etoposide with a $t_{½}$ of 80.8 ± 13.2 min. This finding was apparently contradictory as a lower elimination rate would be expected, when co-administering zosuquidar, like shown in Fig. 5 for the IV administered etoposide. This observation may reflect that the elimination of etoposide was not an ideal first order elimination, and as a result, the elimination rate was underestimated, because C_{max} was significantly lower for this group. For the groups that received oral co-administration of 0.63 mg/kg zosuquidar or more, there was a correlation between the orally co-administered zosuquidar dose and the elimination rate with increasing zosuquidar doses leading to increased $t_{½}$ (Table 3). Thus, increasing doses of orally co-administered zosuquidar of 0.63 mg/kg and above, significantly increased C_{15min} and C_{max}, and correlated with decreased elimination rate. Conclusively, the increased etoposide bioavailability following zosuquidar co-administration was attributed both to increased absorption and decreased elimination of etoposide, which was both mainly attributed to a local intestinal effect elicited by zosuquidar.

3.6. *In vitro-in vivo correlation*

From the present dataset, it was not possible to clarify if doses higher than 63 mg/kg zosuquidar could increase the etoposide bioavailability even further than 35%. As shown in the preformulation precipitation studies, higher zosuquidar doses may precipitate in the intestine, and as an ethanol-water formulation was applied in the present study, it is questionable if higher intestinal zosuquidar concentrations could be achieved. Therefore, an IC_{50} on P-gp function *in vivo*, based on bioavailability cannot be derived exactly. However, at a co-administered dose of 2.0 mg/kg zosuquidar, etoposide bioavailability increased to approximately 22%, which was roughly half of the observed effect between no zosuquidar co-administration (5%) and 63 mg/kg zosuquidar (35%) (Fig. 7). Assuming that the administered volume of oral formulation was immediately diluted in 11 mL/kg fluid in the rat small intestine (McConnell et al., 2008), the concentration of zosuquidar would be approximately 180 μM, where zosuquidar was soluble according to preformulation studies. In Caco-2 monolayers, P-gp activity was reduced by 50% by only 5–10 nM zosuquidar, illustrating that there was a substantial *in vitro-in vivo* discrepancy of at least four orders of magnitude.

The *in vitro-in vivo* correlation above assumes that the entire gastrointestinal tract is a single static compartment with immediate mixing. Obviously, the dynamics of the intestines are more complex than the static *in vitro* system, and the observed discrepancy may in part be ascribed to dilution and unequal distribution of etoposide and zosuquidar along the length of the gastrointestinal tract. Naturally, both etoposide and zosuquidar needed to be at the same location at the same time for zosuquidar to elicit an effect on etoposide absorption. Recently, we showed that oral absorption of the P-gp substrate, digoxin, was increased when a P-gp-inhibiting surfactant and digoxin were adsorbed together on a carrier material (Nielsen et al., 2019). Digoxin absorption was likely enhanced by the co-release of substrate and inhibitor, which resulted in a more even distribution. Additionally, although zosuquidar bioavailability was very low, it may be possible that a relevant amount was absorbed from the intestine and immediately metabolised by first-pass metabolism (Rubin et al., 2002). Hereby, the absorbed and first-pass metabolised amount of zosuquidar would not contribute to the zosuquidar bioavailability, and because it was removed from the small intestine, would not elicit an effect on the oral absorption of etoposide.

4. Conclusions

In the present study, we showed that the P-gp inhibitor, zosuquidar, abolished the polarised permeability of etoposide across Caco-2 monolayers at low nM concentrations. *In vivo*, orally co-administered zosuquidar elicited a low oral bioavailability and increased oral etoposide absorption and decreased etoposide clearance, primarily by limiting intestinal excretion. We estimated that intestinal zosuquidar concentrations in the μM-range were necessary to increase etoposide absorption, which highlighted a substantial *in vitro-in vivo* discrepancy on the effects of zosuquidar on etoposide permeability. The present study provides novel information about *in vitro-in vivo* correlation of intestinal P-gp inhibitor concentrations and substrate bioavailability. Thereby, the study may be useful for future study designs or formulation development using zosuquidar to increase bioavailability of etoposide or other poorly permeable P-gp substrates.

Author contributions

Conception and design of the study: RBN, RH, IP, JS, UGN, and CUN. Acquisition of data: RBN, RH, IP. Analysis and interpretation of data: RBN, RH, IP, JS, UGN, and CUN. Drafting the manuscript: RBN, RH, and CUN. Critical revising and final approval of the version submitted: RBN, RH, IP, JS, UGN, and CUN.

Declaration of Competing Interest

The authors declare that they have no known competing financial og personal interests.

Acknowledgements

Researchers and technicians at Janssen Pharmaceutica and The University of Southern Denmark who helped design and conduct various studies, including Maria Læssøe Pedersen, Dries Versweyveld, Lieve Dillen, Annemie Noels, Dirk Roelant, and Kathleen Allaerts, are hereby acknowledged.

References

Adane, E.D., Liu, Z., Xiang, T.-X., Anderson, B.D., Leggas, M., 2012. Pharmacokinetic modeling to assess factors affecting the oral bioavailability of the lactone and carboxylate forms of the lipophilic camptothecin analogue AR-67 in rats. Pharm. Res. 29, 1722–1736. https://doi.org/10.1007/s11095-011-0617-0.

Al-Ali, A.A.A., Quach, J.R.C., Bundgaard, C., Steffansen, B., Holm, R., Nielsen, C.U., 2018a. Polysorbate 20 alters the oral bioavailability of etoposide in wild type and mdr1a deficient Sprague-Dawley rats. Int. J. Pharm. 543, 352–360. https://doi.org/10.1016/j.ijpharm.2018.04.006.

Al-Ali, A.A.A., Steffansen, B., Holm, R., Nielsen, C.U., 2018b. Nonionic surfactants increase digoxin absorption in Caco-2 and MDCKII MDR1 cells: impact on P-glycoprotein inhibition, barrier function, and repeated cellular exposure. Int. J. Pharm. 551, 270–280. https://doi.org/10.1016/j.ijpharm.2018.09.039.

Al-Ali, A.A.A., Sandra, L., Versweyveld, D., Pijpers, I., Dillen, L., Vermeulen, A., Snoeys, J., Holm, R., Nielsen, C.U., 2020. High-dose etoposide formulations do not saturate intestinal P-glycoprotein: development, stability, and pharmacokinetics in Sprague-Dawley rats. Int. J. Pharm. 583, 119399. https://doi.org/10.1016/j.ijpharm.2020.119399.

Alam, A., Kung, R., Kowal, J., McLeod, R.A., Tremp, N., Broude, E.V., Roninson, I.B., Stahlberg, H., Locher, K.P., 2018. Structure of a zosuquidar and UIC2-bound human-mouse chimeric ABCB1. Proc. Natl. Acad. Sci. U. S. A. 115, E1973–E1982. https://doi.org/10.1073/pnas.1717044115.

Alam, A., Kowal, J., Broude, E., Roninson, I., Locher, K.P., 2019. Structural insight into substrate and inhibitor discrimination by human P-glycoprotein. Science 363, 753–756. https://doi.org/10.1126/science.aav7102.

American Veterinary Medical Association, 2020. AVMA Guidelines for the Euthanasia of Animals: 2020 Edition. Accessed May 12 2021. https://www.avma.org/sites/default/files/2020-01/2020-Euthanasia-Final-1-17-20.pdf.

Anderson, B.D., May, M.J., Jordan, S., Song, L., Roberts, M.J., Leggas, M., 2006. Dependence of nelfinavir brain uptake on dose and tissue concentrations of the selective P-glycoprotein inhibitor zosuquidar in rats. Drug Metab. Dispos. 34, 653–659. https://doi.org/10.1124/dmd.105.006536.

Bardelmeijer, H.A., Ouwehand, M., Beijnen, J.H., Schellens, J.H.M., van Tellingen, O., 2004. Efficacy of novel P-glycoprotein inhibitors to increase the oral uptake of paclitaxel in mice. Investig. New Drugs 22, 219–229. https://doi.org/10.1023/b:Drug.0000026248.45084.21.

Berghausen, J., Seiler, F.H., Gobeau, N., Faller, B., 2016. Simulated rat intestinal fluid improves oral exposure prediction for poorly soluble compounds over a wide dose range. Admet and Dmpk 4, 35–53. https://doi.org/10.5599/admet.4.1.258.

Bihorel, S., Camenisch, G., Lemaire, M., Scherrmann, J.-M., 2007. Influence of breast cancer resistance protein (Abcg2) and p-glycoprotein (Abcb1a) on the transport of imatinib mesylate (Gleevec((R))) across the mouse blood-brain barrier. J. Neurochem. 102, 1749–1757. https://doi.org/10.1111/j.1471-4159.2007.04808.x.

Chen, Y., Agarwal, S., Shaik, N.M., Chen, C., Yang, Z., Elmquist, W.F., 2009. P-glycoprotein and Breast Cancer Resistance Protein Influence Brain distribution of Dasatinib. J. Pharmacol. Exp. Ther. 330, 956–963. https://doi.org/10.1124/jpet.109.154781.

Choo, E.F., Leake, B., Wandel, C., Imamura, H., Wood, A.J.J., Wilkinson, G.R., Kim, R.B., 2000. Pharmacological inhibition of P-glycoprotein transport enhances the distribution of HIV-1 protease inhibitors into brain and testes. Drug Metab. Dispos. 28, 655–660.

Cripe, L.D., Uno, H., Paietta, E.M., Litzow, M.R., Ketterling, R.P., Bennett, J.M., Rowe, J. M., Lazarus, H.M., Luger, S., Tallman, M.S., 2010. Zosuquidar, a novel modulator of P-glycoprotein, does not improve the outcome of older patients with newly diagnosed acute myeloid leukemia: a randomized, placebo-controlled trial of the Eastern Cooperative Oncology Group 3999. Blood 116, 4077–4085. https://doi.org/10.1182/blood-2010-04-277269.

Dai, H.Q., Marbach, P., Lemaire, M., Hayes, M., Elmquist, W.F., 2003. Distribution of STI-571 to the brain is limited by P-glycoprotein-mediated efflux. J. Pharmacol. Exp. Ther. 304, 1085–1092. https://doi.org/10.1124/jpet.102.045260.

Dantzig, A.H., Shepard, R.L., Cao, J., Law, K.L., Ehlhardt, W.J., Baughman, T.M., Bumol, T.F., Starling, J.J., 1996. Reversal of P-glycoprotein-mediated multidrug resistance by a potent cyclopropyldibenzosuberane modulator, LY335979. Cancer Res. 56, 4171–4179.

Delp, M.D., Evans, M.V., Duan, C.P., 1998. Effects of aging on cardiac output, regional blood flow, and body composition in Fischer-344 rats. J. Appl. Physiol. 85, 1813–1822. https://doi.org/10.1152/jappl.1998.85.5.1813.

Dou, L., Gavins, F.K.H., Mai, Y., Madla, C.M., Taherali, F., Orlu, M., Murdan, S., Basit, A. W., 2020. Effect of food and an animal's sex on p-glycoprotein expression and luminal fluids in the gastrointestinal tract of wistar rats. Pharmaceutics 12, 296. https://doi.org/10.3390/pharmaceutics12040296.

Drugbank, 2021. Zosuquidar. Accessed May 11th 2021. https://go.drugbank.com/drugs/DB06191.

Ehlhardt, W.J., Woodland, J.M., Baughman, T.M., Vandenbranden, M., Wrighton, S.A., Kroin, J.S., Norman, B.H., Maple, S.R., 1998. Liquid chromatography nuclear magnetic resonance spectroscopy and liquid chromatography mass spectrometry identification of novel metabolites of the multidrug resistance modulator LY335979 in rat bile and human liver microsomal incubations. Drug Metab. Dispos. 26, 42–51.

Fracasso, P.M., Goldstein, L.J., de Alwis, D.P., Rader, J.S., Arquette, M.A., Goodner, S.A., Wright, L.P., Fears, C.L., Gazak, R.J., Andre, V.A.M., Burgess, M.F., Slapak, C.A., Schellens, J.H.M., 2004. Phase I study of docetaxel in combination with the P-glycoprotein inhibitor, zosuquidar, in resistant malignancies. Clin. Cancer Res. 10, 7220–7228. https://doi.org/10.1158/1078-0432.Ccr-04-0452.

Gerrard, G., Payne, E., Baker, R.J., Jones, D.T., Potter, M., Prentice, H.G., Ethell, M., McCullough, H., Burgess, M., Mehta, A.B., Ganeshaguru, K., 2004. Clinical effects and P-glycoprotein inhibition in patients with acute myeloid leukemia treated with zosuquidar trihydrochloride, daunorubicin and cytarabine. Haematologica 89, 782–790.

Green, L.J., Marder, P., Slapak, C.A., 2001. Modulation by LY335979 of P-glycoprotein function in multidrug-resistant cell lines and human natural killer cells. Biochem. Pharmacol. 61, 1393–1399. https://doi.org/10.1016/s0006-2952(01)00599-8.

Guo, A., Marinaro, W., Hu, P.D., Sinko, P.J., 2002. Delineating the contribution of secretory transporters in the efflux of etoposide using Madin-Darby canine kidney (MDCK) cells overexpressing P-glycoprotein (Pgp), multidrug resistance-associated protein (MRP1), and canalicular multispecific organic anion transporter (cMOAT)4. Drug Metab. Dispos. 30, 457–463. Unsp 543/97388. https://doi.org/10.1124/dmd.30.4.457.

Heredi-Szabo, K., Palm, J.E., Andersson, T.B., Pal, A., Mehn, D., Fekete, Z., Beery, E., Jakab, K.T., Jani, M., Krajcsi, P., 2013. A P-gp vesicular transport inhibition assay - Optimization and validation for drug-drug interaction testing. Eur. J. Pharm. Sci. 49, 773–781. https://doi.org/10.1016/j.ejps.2013.04.032.

Kara, Z.P., Civelek, D.O., Ozturk, N., Okyar, A., 2021. The effects of P-glycoprotein inhibitor zosuquidar on the sex and time-dependent pharmacokinetics of parenterally administered talinolol in mice. Eur. J. Pharm. Sci. 156, 105589 https://doi.org/10.1016/j.ejps.2020.105589.

Karssen, A.M., Meijer, O.C., van der Sandt, I.C.J., De Boer, A.G., De Lange, E.C.M., De Kloet, E.R., 2002. The role of the efflux transporter P-glycoprotein in brain penetration of prednisolone. J. Endocrinol. 175, 251–260. https://doi.org/10.1677/joe.0.1750251.

Kono, Y., Kawahara, I., Shinozaki, K., Nomura, I., Marutani, H., Yamamoto, A., Fujita, T., 2021. Characterization of P-Glycoprotein Inhibitors for evaluating the effect of P-Glycoprotein on the Intestinal Absorption of drugs. Pharmaceutics 13, 388. https://doi.org/10.3390/pharmaceutics13030388.

Kwak, J.-O., Lee, S.H., Lee, G.S., Kim, M.S., Ahn, Y.-G., Lee, J.H., Kim, S.W., Kim, K.H., Lee, M.G., 2010. Selective inhibition of MDR1 (ABCB1) by HM30181 increases oral bioavailability and therapeutic efficacy of paclitaxel. Eur. J. Pharmacol. 627, 92–98. https://doi.org/10.1016/j.ejphar.2009.11.008.

Lagas, J.S., Fan, L., Wagenaar, E., Vlaming, M.L.H., van Tellingen, O., Beijnen, J.H., Schinkel, A.H., 2010. P-glycoprotein (P-gp/Abcb1), Abcc2, and Abcc3 Determine the Pharmacokinetics of Etoposide. Clin. Cancer Res. 16, 130–140. https://doi.org/10.1158/1078-0432.Ccr-09-1321.

Lancet, J.E., Baer, M.R., Duran, G.E., List, A.F., Fielding, R., Marcelletti, J.F., Multani, P. S., Sikic, B.I., 2009. A phase I trial of continuous infusion of the multidrug resistance inhibitor zosuquidar with daunorubicin and cytarabine in acute myeloid leukemia. Leuk. Res. 33, 1055–1061. https://doi.org/10.1016/j.leukres.2008.09.015.

Le, L.H., Moore, M.J., Siu, L.L., Oza, A.M., MacLean, M., Fisher, B., Chaudhary, A., de Alwis, D.P., Slapak, C., Seymour, L., 2005. Phase I study of the multidrug resistance inhibitor zosuquidar administered in combination with vinorelbine in patients with advanced solid tumours. Cancer Chemother. Pharmacol. 56, 154–160. https://doi.org/10.1007/s00280-004-0942-7.

Lehnert, M., de Giuli, R., Kunke, K., Emerson, S., Dalton, W.S., Salmon, S.E., 1996. Serum can inhibit reversal of multidrug resistance by chemosensitisers. Eur. J. Cancer 32a, 862–867. https://doi.org/10.1016/0959-8049(96)00004-4.

Ludescher, C., Eisterer, W., Hilbe, W., Hofmann, J., Thaler, J., 1995. Decreased potency of MDR-modulators under serum conditions determined by a functional assay. Br. J. Haematol. 91, 652–657. https://doi.org/10.1111/j.1365-2141.1995.tb05362.x.

Mai, Y., Dou, L., Murdan, S., Basit, A.W., 2018. An animal's sex influences the effects of the excipient PEG 400 on the intestinal P-gp protein and mRNA levels, which has implications for oral drug absorption. Eur. J. Pharm. Sci. 120, 53–60. https://doi.org/10.1016/j.ejps.2018.04.021.

Mai, Y., Dou, L., Madla, C.M., Murdan, S., Basit, A.W., 2019. Sex-dependence in the effect of pharmaceutical excipients: polyoxyethylated solubilising excipients increase oral drug bioavailability in male but not female rats. Pharmaceutics 11, 228. https://doi.org/10.3390/pharmaceutics11050228.

Mai, Y., Dou, L., Yao, Z.C., Madla, C.M., Gavins, F.K.H., Taherali, F., Yin, H.Y., Orlu, M., Murdan, S., Basit, A.W., 2021. Quantification of P-Glycoprotein in the Gastrointestinal Tract of Humans and Rodents: Methodology, Gut Region, sex, and Species Matter. Mol. Pharm. 18, 1895–1904. https://doi.org/10.1021/acs.molpharmaceut.0c00574.

Makhey, V.D., Guo, A.L., Norris, D.A., Hu, P.D., Yan, J.S., Sinko, P.J., 1998. Characterization of the regional intestinal kinetics of drug efflux in rat and human intestine and in Caco-2 cells. Pharm. Res. 15, 1160–1167. https://doi.org/10.1023/a:1011971303880.

Matsuda, Y., Konno, Y., Hashimoto, T., Nagai, M., Taguchi, T., Satsukawa, M., Yamashita, S., 2013. In Vivo assessment of the impact of efflux transporter on oral drug absorption using portal vein-cannulated rats. Drug Metab. Dispos. 41, 1514–1521. https://doi.org/10.1124/dmd.113.051680.

McConnell, E.L., Basit, A.W., Murdan, S., 2008. Measurements of rat and mouse gastrointestinal pH fluid and lymphoid tissue, and implications for in-vivo experiments. J. Pharm. Pharmacol. 60, 63–70. https://doi.org/10.1211/jpp.60.1.0008.

Mittapalli, R.K., Vaidhyanathan, S., Sane, R., Elmquist, W.F., 2012. Impact of P-glycoprotein (ABCB1) and breast cancer resistance protein (ABCG2) on the brain distribution of a novel BRAF inhibitor: Vemurafenib (PLX4032). J. Pharmacol. Exp. Ther. 342, 33–40. https://doi.org/10.1124/jpet.112.192195.

Morschhauser, F., Zinzani, P.L., Burgess, M., Sloots, L., Bouafia, F., Dumontet, C., 2007. Phase I/II trial of a P-glycoprotein inhibitor, Zosuquidar. 3HCl trihydrochloride (LY335979), given orally in combination with the CHOP regimen in patients with non-Hodgkin's lymphoma. Leuk. Lymphoma 48, 708–715. https://doi.org/10.1080/10428190701190169.

Mouly, S.J., Paine, M.F., Watkins, P.B., 2004. Contributions of CYP3A4, P-glycoprotein, and serum protein binding to the intestinal first-pass extraction of saquinavir. J. Pharmacol. Exp. Ther. 308, 941–948. https://doi.org/10.1124/jpet.103.056390.

Nagaya, Y., Katayama, K., Kusuhara, H., Nozaki, Y., 2020. Impact of P-glycoprotein-mediated active efflux on drug distribution into lumbar cerebrospinal fluid in nonhuman primates. Drug Metab. Dispos. 48, 1183–1190. https://doi.org/10.1124/dmd.120.000099.

Nielsen, R.B., Kahnt, A., Dillen, L., Wuyts, K., Snoeys, J., Nielsen, U.G., Holm, R., Nielsen, C.U., 2019. Montmorillonite-surfactant hybrid particles for modulating intestinal P-glycoprotein-mediated transport. Int. J. Pharm. 571, 118696. https://doi.org/10.1016/j.ijpharm.2019.118696.

Nosol, K., Romane, K., Irobalieva, R.N., Alam, A., Kowal, J., Fujita, N., Locher, K.P., 2020. Cryo-EM structures reveal distinct mechanisms of inhibition of the human multidrug transporter ABCB1. Proc. Natl. Acad. Sci. U. S. A. 117, 26245–26253. https://doi.org/10.1073/pnas.2010264117.

Ozgur, B., Saaby, L., Langthaler, K., Brodin, B., 2018a. Characterization of the IPEC-J2 MDR1 (iP-gp) cell line as a tool for identification of P-gp substrates. Eur. J. Pharm. Sci. 112, 112–121. https://doi.org/10.1016/j.ejps.2017.11.007.

Ozgur, B., Saaby, L., Langthaler, K., Brodin, B., 2018b. Data demonstrating the challenges of determining the kinetic parameters of P-gp mediated transport of low-water soluble substrates. Data Brief 16, 655–659. https://doi.org/10.1016/j.dib.2017.11.092.

Paek, I.B., Ji, H.Y., Kim, M.S., Lee, G.S., Lee, H.S., 2006. Simultaneous determination of paclitaxel and a new P-glycoprotein inhibitor HM-30181 in rat plasma by liquid chromatography with tandem mass spectrometry. J. Sep. Sci. 29, 628–634. https://doi.org/10.1002/jssc.200500368.

Rubin, E.H., de Alwis, D.P., Pouliquen, I., Green, L., Marder, P., Lin, Y., Musanti, R., Grospe, S.L., Smith, S.L., Toppmeyer, D.L., Much, J., Kane, M., Chaudhary, A., Jordan, C., Burgess, M., Slapak, C.A., 2002. A phase I trial of a potent P-glycoprotein inhibitor, zosuquidar.3HCl trihydrochloride (LY335979), administered orally in combination with doxorubicin in patients with advanced malignancies. Clin. Cancer Res. 8, 3710–3717.

Ruff, P., Vorobiof, D.A., Jordaan, J.P., Demetriou, G.S., Moodley, S.D., Nosworthy, A.L., Werner, I.D., Raats, J., Burgess, L.J., 2009. A randomized, placebo-controlled, double-blind phase 2 study of docetaxel compared to docetaxel plus zosuquidar (LY335979) in women with metastatic or locally recurrent breast cancer who have received one prior chemotherapy regimen. Cancer Chemother. Pharmacol. 64, 763–768. https://doi.org/10.1007/s00280-009-0925-9.

Sandler, A., Gordon, M., de Alwis, D.P., Pouliquen, I., Green, L., Marder, P., Chaudhary, A., Fife, K., Battiato, L., Sweeney, C., Jordan, C., Burgess, M., Slapak, C. A., 2004. A phase I trial of a potent P-glycoprotein inhibitor, zosuquidar trihydrochloride (LY335979), administered intravenously in combination with doxorubicin in patients with advanced malignancy. Clin. Cancer Res. 10, 3265–3272. https://doi.org/10.1158/1078-0432.Ccr-03-0644.

Shaik, N., Giri, N., Pan, G., Elmquist, W.F., 2007. P-glycoprotein-mediated active efflux of the anti-HIV1 nucleoside abacavir limits cellular accumulation and brain distribution. Drug Metab. Dispos. 35, 2076–2085. https://doi.org/10.1124/dmd.107.017723.

Slate, D.L., Bruno, N.A., Casey, S.M., Zutshi, N., Garvin, L.J., Wu, H., Pfister, J.R., 1995. RS-33295-198: a novel, potent modulator of P-glycoprotein-mediated multidrug resistance. Anticancer Res. 15, 811–814.

Smolinski, M.P., Urgaonkar, S., Pitzonka, L., Cutler, M., Lee, G., Suh, K.H., Lau, J.Y.N., 2021. Discovery of encequidar, first-in-class intestine specific P-glycoprotein inhibitor. J. Med. Chem. https://doi.org/10.1021/acs.jmedchem.0c01826.

Troutman, M.D., Thakker, D.R., 2003. Efflux ratio cannot assess P-glycoprotein-mediated attenuation of absorptive transport: asymmetric effect of P-glycoprotein on absorptive and secretory transport across Caco-2 cell monolayers. Pharm. Res. 20, 1200–1209. https://doi.org/10.1023/a:1025049014674.

Tsukimoto, M., Ohashi, R., Torimoto, N., Togo, Y., Suzuki, T., Maeda, T., Kagawa, Y., 2015. Effects of the inhibition of intestinal P-glycoprotein on aliskiren pharmacokinetics in cynomolgus monkeys. Biopharm. Drug Dispos. 36, 15–33. https://doi.org/10.1002/bdd.1920.